Sensors and Actuators B 177 (2013) 145–152

Contents lists available at SciVerse ScienceDirect

Sensors and Actuators B: Chemical

journal homepage: www.elsevier.com/locate/snb

Assembly of layered double hydroxide/ANTS ultrathin film and its application as a biosensing material

Lan Jin, Zhijie Guo, Tengli Wang, Min Wei*

State Key Laboratory of Chemical Resource Engineering, Beijing University of Chemical Technology, Beijing 100029, China

ARTICLE INFO

Article history:
Received 7 August 2012
Received in revised form 12 October 2012
Accepted 22 October 2012
Available online xxx

Keywords:
Layered double hydroxide
ANTS
Ultrathin film
Biosensor
Dextran-40

ABSTRACT

The fluorescent ultrathin films (UTFs) based on layered double hydroxide/8-amino-1,3,6-naphthalenetrisulfonate (LDH/ANTS) have been prepared by employing a layer-by-layer assembly technique, and its application as an optical biosensor for dextran-40 was demonstrated. UV–vis spectroscopy, fluorescence spectroscopy, X-ray diffraction, scanning electron microscopy and atomic force microscopy have been adopted to monitor the assembly process. The UTFs display a continuous and uniform morphology, with a long-range ordered structure. It was found that the UTFs can be used for dextran-40 sensing in the concentration range 1.0×10^{-5} to 1.0×10^{-2} M, and the detection limit of 2.7×10^{-6} M is obtained. Good selectivity toward dextran-40 over other saccharides, including glucose, fructose and sucrose, has been demonstrated. Furthermore, the UTFs show a good reusable ability for dextran-40 by recovering the UTFs in a H_2O_2 aqueous solution (1.0×10^{-4} M), with the relative standard deviation of 4.18% toward dextran-40 for 10 cycles. The fluorescence response of the film sensor is attributed to a strong interaction between ANTS and dextran-40, which was verified by XPS, Raman and polarized photoemission spectroscopy, accounting for the significant fluorescence quenching of the LDH/ANTS film. The results indicate that the LDH/ANTS UTFs in this work can be used as a biosensor for the detection of dextran-40.

1. Introduction

Saccharides are one of the most abundant biomolecules, which are essential in life processes, and play fundamental roles in controlling an individual's birth, differentiation and immunity [1]. Owing to their wide usages and special activities in biological processes, recognition of saccharides by the synthetic hosts is of considerable interest [2]. In particular, achieving sufficient sensitivity and selectivity for practical clinical uses is a challenging task because of their structural diversity. At present, there has been a great deal of interest in developing the oligosaccharides chemosensor by using the fluorescence compound. For instance, anthrylboronic acid has been used for sugar sensor via a fluorescence quenching process [3]. The tetraphenylethene-boronic acid complex has been synthesized and its biosensor specificity for D-glucose was studied [4]. Shinkai et al. have developed the sensors for precise and selective sugar recognition [5]. Later, Sukhorukov et al. investigated the possibility of using phenylboronic acid grafted poly(acrylic acid)-mannan to prepare thin films and hollow capsules which are very sensitive to several carbohydrates [6]. Recently, designing the interesting methods for saccharide sensors with more sensitive and selective has been reported [7,8]. A hybrid complex of curdlan with polythiophene functioned as a highly sensitive and selective saccharide sensor has also been demonstrated [9].

Despite all these progress in detecting the oligosaccharides, several problems remain not-well resolved. Firstly, most of sensors response can only be realized at pH 9 or a higher pH condition, which are not available in vivo. Secondly, there are a limited number of oligosaccharide sensors that can be used for rapid sample analysis, and this strategy may have some limitations when extended to higher oligosaccharides. Dextran-40, with the degree of polymerization 40, has been widely used in medicine as a blood plasma volume expander or blood flow improver for many years [10,11]. However, the highly selective detection and recognition of dextran-40 in complex media is a key challenge in diagnostics, industrial and biotechnological applications [12], especially under the physiological conditions.

8-Amino-1,3,6-naphthalenetrisulfonate (ANTS) is a naphthalene derivative dye that has been used for labeling the protein in electrophoresis [13] and detecting oligosaccharides [14]. However, most previous work is focused on detection of oligosaccharides in ANTS solution, which limits its practical application. In addition, ANTS molecule suffers from long-term sustainability as the result of variation in temperature, environmental pH, etc. Therefore, it is of great significance to design and fabricate ANTS-based fluorescence

* Corresponding author. Tel.: +86 10 64412131; fax: +86 10 64425385.
E-mail address: weimin@mail.buct.edu.cn (M. Wei).

0925-4005/$ – see front matter © 2012 Elsevier B.V. All rights reserved.
http://dx.doi.org/10.1016/j.snb.2012.10.105

chemosensors, which can meet the demands of high selectivity, cycling stability as well as biocompatibility under physiological conditions. Layered double hydroxides (LDHs) are important 2-dimensional clay with anion-exchange properties, which have been widely used as catalysts and supports [15,16], separation technology [17], and host matrix for functional compounds [18,19]. Recently, the delamination of LDHs into nanosheets and preparation of inorganic/organic fluorophore ultrathin films have been reported [20,21]. This inspires us to take the challenge of incorporating ANTS into LDH host matrix for achieving a new chemosensor for the detection of dextran-40, which may exhibit the following advantages: the LDH nanosheets offer a confined environment for ANTS, which can enhance the optical and thermal stability of ANTS; Immobilization ANTS by LDH also allows for sensor regeneration and can be engineered to improve the sensor performance.

In this paper, the LDH/ANTS UTFs have been assembled through layer by layer techniques. The obtained nanocomposite films display a uniform morphology with a long-range ordered structure, and can be utilized as a fluorescence chemosensor for the detection of dextran oligosaccharides (dextran-40) with rather high selectivity. Furthermore, the LDH/ANTS UTFs show the advantages of easy regeneration and recycle ability for long-term employment, resulting from the interaction of UTFs with H_2O_2 by the reductive amination reaction. To the best of our knowledge, the detection and measurement of dextran-40 by a solid film chemosensor has not yet been reported so far. Therefore, the LDH/ANTS UTFs can provide high sensitivity and selectivity for label-free, rapid, low-cost detection of dextran-40, which can be potentially used in clinical diagnostics and biotechnology.

2. Experimental

2.1. Materials

8-Amino-1,3,6-naphthalenetrisulfonate sodium salt was purchased from J&K Scientific Ltd. Dextran-40, glucose, fructose, and sucrose was purchased from Sangon Biotech Co. of Shanghai (China). The analytical grade chemicals including $Zn(NO_3)_2{\cdot}6H_2O$, $Al(NO_3)_3{\cdot}9H_2O$, NaOH, H_2O_2 and other nitrate salts of metal ion were used without further purification. The deionized and decarbonated water was used in all experimental processes.

2.2. Fabrication of the $(LDH/ANTS)_n$ UTFs

The Zn_2Al–NO_3 LDH precursor was synthesized by the hydrothermal method reported previously [22]. Then a 0.1 g of Zn_2Al–NO_3 LDH was shaken in 100 mL of formamide solution for 24 h to obtain a colloidal suspension of exfoliated Zn_2Al-LDH nanosheets. The quartz glass substrate was cleaned in concentrated NH_3:H_2O_2 (v/v:7:3) and concentrated H_2SO_4 for 30 min, respectively. Thereafter, the surface of substrates was hydrophilic and negatively charged. The quartz substrate was rinsed and washed thoroughly with deionized water before use. The multilayer films composed of LDH nanosheets and ANTS molecule were fabricated on pretreated quartz glass substrate through the LBL technique. The substrate was dipped in a colloidal suspension (0.1 g/mL) of LDH nanosheets for 10 min and washed thoroughly with deionized water. Then the substrate was immersed into an aqueous solution of ANTS (0.2 g/mL) for another 10 min followed by washing. Subsequently, the deposition operation for LDH nanosheets and ANTS was repeated n times to obtain a multilayer film of $(LDH/ANTS)_n$. The resulting films were dried with a nitrogen gas flow for 2 min at 25 °C.

2.3. The response of dextran-40 measurement

The dextran-40 solutions with the different concentrations were prepared by dissolving the dextran-40 solid in water. The fluorescence chemosensor of LDH/ANTS UTF was immersed into a quartz cell with dextran-40 solution, and its response was recorded by a RF-5301PC fluorophotometer with a liquid holder based on the fluorescence quenching as a function of the dextran-40 concentration.

2.4. Techniques of characterization

The UV–vis absorption measurements were performed on a Shimadzu UV-2501PC spectrometer. Fluorescence emission spectra were recorded on a RF-5301PC fluorophotometer in the range 400–650 nm with the excitation wavelength of 365 nm and a slit width of 5 nm. The morphology and thickness of the thin film were investigated by using a ZEISS scanning electron microscope (SEM). The surface roughness data were obtained by using the atomic force microscopy (AFM) software (Digital Instruments, Version 6.12). X-ray diffraction patterns (XRD) measurements were performed on a Rigaku XRD-6000 diffractometer, using Cu Kα radiation (λ = 0.15418 nm) at 40 kV, 30 mA, with a scanning rate of 10 min^{-1}, and the 2θ angle ranging from 2° to 10°. Steady-state polarized photoluminescence measurements of the LDH/ANTS UTFs were recorded with an Edinburgh Instruments' FLS 920 fluorospectrophotometer. X-ray photoelectron spectroscopy (XPS) measurement was performed with monochromatized A1 Kα exciting X-radiation (PHI Quantera SXM). Raman spectra were measured with Renishaw-inVia Raman microscope.

3. Results and discussion

3.1. Assembly of the $(LDH/ANTS)_n$ UTFs

The assembling process of the $(LDH/ANTS)_n$ UTFs was monitored by UV–vis absorption spectra of quartz substrates coated with $(ZnAl\text{-}LDH/ANTS)_n$ (Fig. 1A, n varies from 2 to 20). The inset in Fig. 1A shows that the intensities of the absorption bands at ~222 nm attributed to ANTS increase linearly as a function of bilayer number n, indicating a regular and uniform growth of the UTFs. A wavelength shift of ANTS was observed compared with its counterpart in aqueous solution (220 nm, dashed line in Fig. 1A), as a result of the electrostatic interaction between ANTS and LDH nanosheets. Fig. 1B shows the fluorescence spectra of the LDH/ANTS UTFs with different n (5–40), from which the $(LDH/ANTS)_{20}$ and $(LDH/ANTS)_{40}$ UTF display the strongest fluorescence intensity. Therefore, the film with n = 20 was chosen as the optimum sample in the following section.

3.2. The surface morphology and structure of the $(LDH/ANTS)_n$ UTFs

The SEM images (Figs. 2A and S1) show the surface smoothness and uniformity of the UTFs decrease with the increase of bilayer number. The thickness of $(LDH/ANTS)_{20}$ UTF is 41 nm observed from its side view of the SEM image (Fig. 2B), from which it can be estimated that the thickness of one bilayer $(LDH/ANTS)_1$ is ~2.05 nm. Taking into account the dimension of ANTS molecule (0.79 nm calculated by Gaussian 03) and the basal distance of LDH/ANTS thin film, it can be speculated that ANTS molecules adopt a double-layered arrangement model. The schematic structures of LDH/ANTS UTFs were tentatively proposed and presented in Scheme 1A.

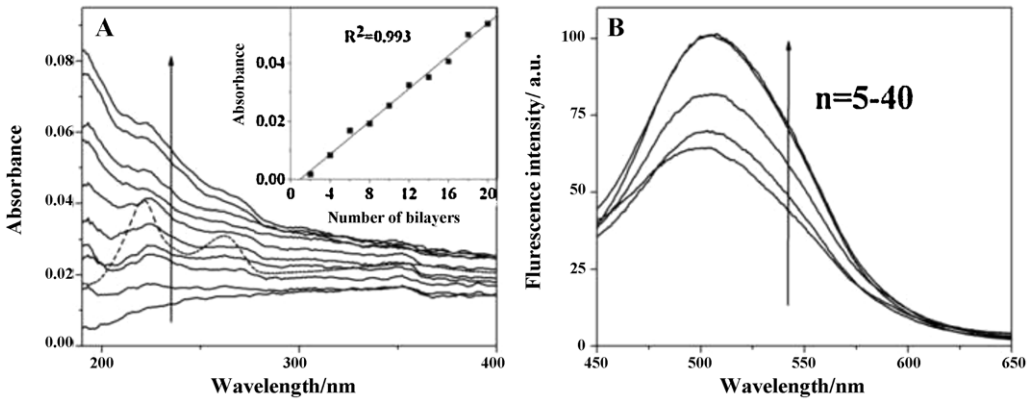

Fig. 1. (A) UV–vis absorption spectra of the $(LDH/ANTS)_n$ UTFs assembled on quartz substrates (The dashed line shows the absorption of ANTS in aqueous solution. Inset: the linear relationship between absorbance at 222 nm and bilayer number n). (B) Emission spectra of the $(LDH/ANTS)_n$ UTFs assembled on quartz substrates (n = 5, 10, 15, 20 and 40, respectively).

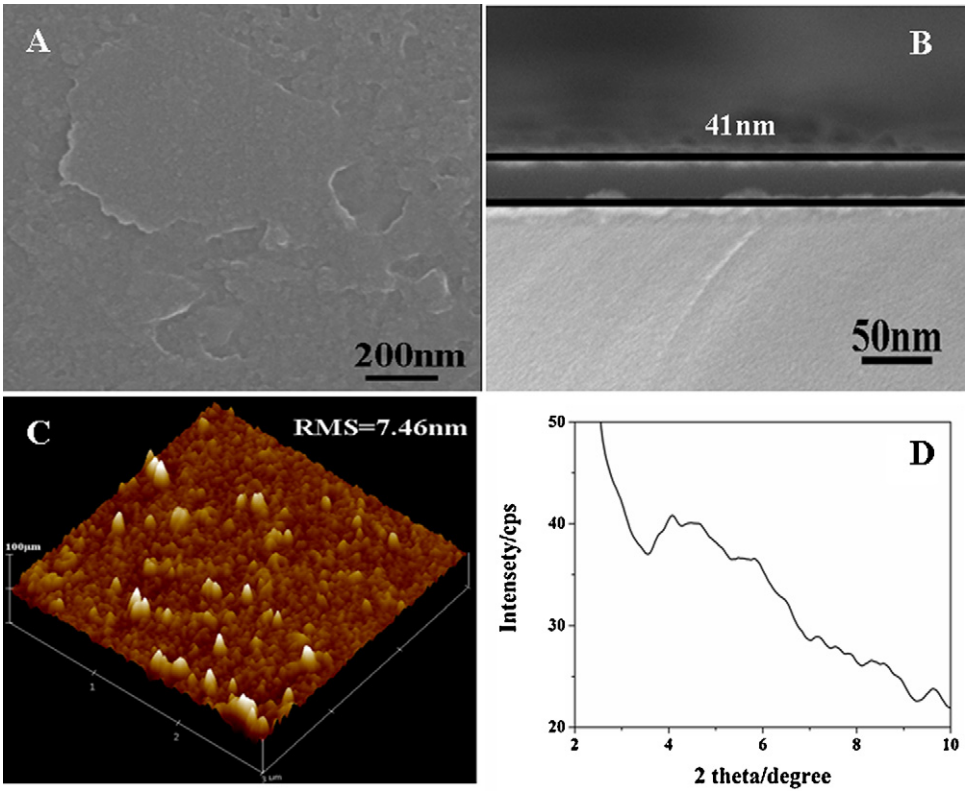

Fig. 2. (A) Top-view of SEM image, (B) side-view of SEM image, (C) tapping-mode AFM image and (D) XRD pattern for the $(LDH/ANTS)_{20}$ UTF.

The deposition process of the $(LDH/ANTS)_n$ UTFs was further monitored by scanning electron microscopy (Fig. S2). The thickness of the as-prepared UTFs (n = 5–20) are in the range of 13–41 nm. The approximately linear increase of the thickness upon increasing the layer number confirms that the UTFs present uniform and periodic layered structure, which is in agreement with the behavior revealed by the absorption and fluorescence spectra above.

The AFM topographical images (Figs. 2C and S3) show the value of root-mean square roughness (RSM) increases from 2.82 nm (n = 5) to 7.46 nm (n = 20), indicating the decrease in uniformity of the UTFs along with the assembly of LBL films. The XRD patterns (Fig. 2D) exhibit a Bragg peak at $2\theta = 4.07^\circ$. The average repeating distance is ~2.17 nm, approximately consistent with the thickness augment per deposited cycle observed by SEM (2.05 nm).

3.3. The $(LDH/ANTS)_{20}$ UTF as fluorescence chemosensors for dextran-40

3.3.1. Effect of pH

For many biological applications, it is very important that the sensor can be used in the physiological pH range. The fluorescence intensity of $(LDH/ANTS)_{20}$ UTF in the absence and presence of dextran-40 at various pH values were measured. As can be seen from Fig. 3, the emission intensity (505 nm) of $(LDH/ANTS)_{20}$ UTF remains almost constant over a broad pH range 5.5–9.0 (curve *a*). In the present of dextran-40, a significant florescence quenching was observed (curve *b*), with a stable intensity in the whole pH range. The results indicate that the LDH/ANTS UTF maintains good fluorescence sensing ability toward dextran-40 over a rather wide pH range, which is the most distinct feature for the environmental

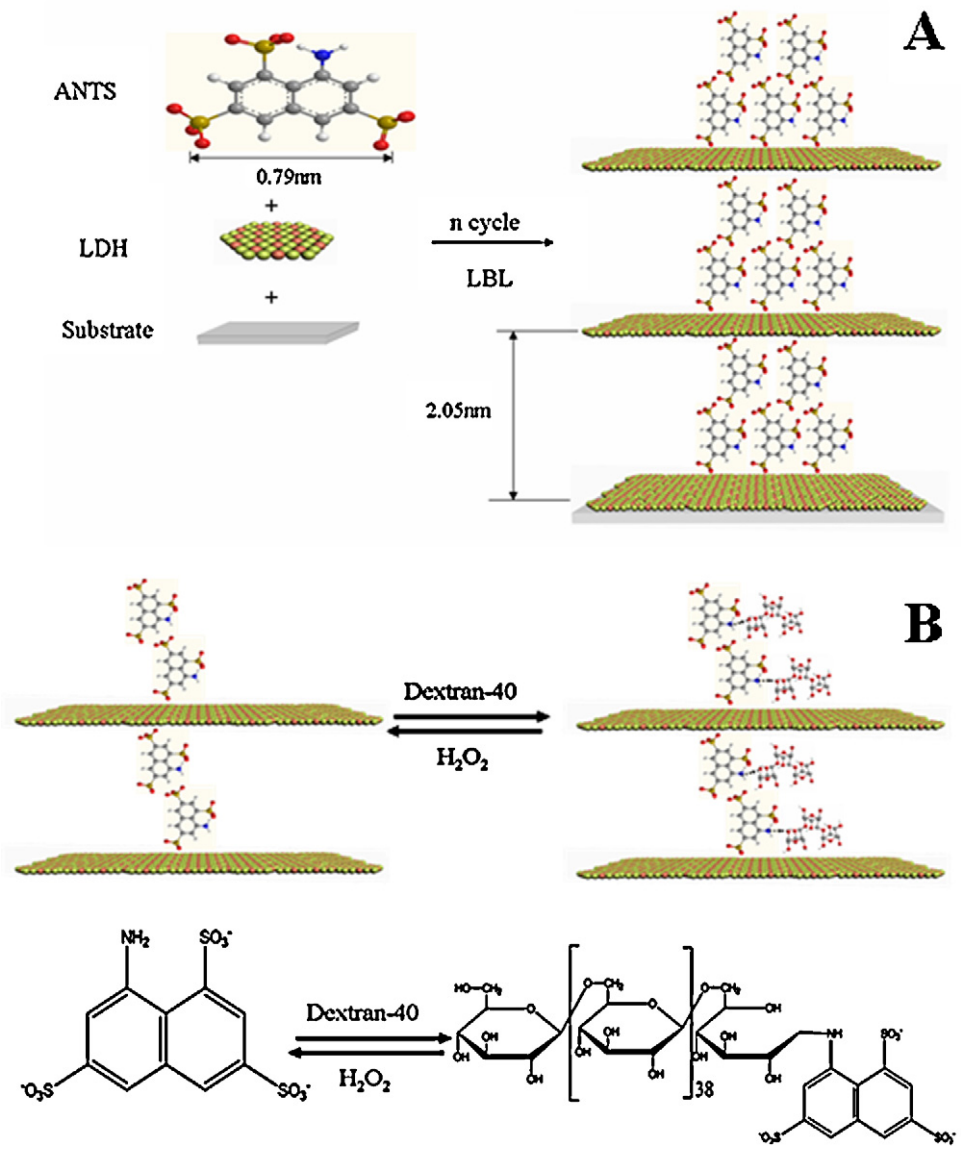

Scheme 1. (A) A possible structure representation of the LDH/ANTS UTF and (B) the mechanism for the measurement-regeneration cycle of the LDH/ANTS UTF with dextran-40.

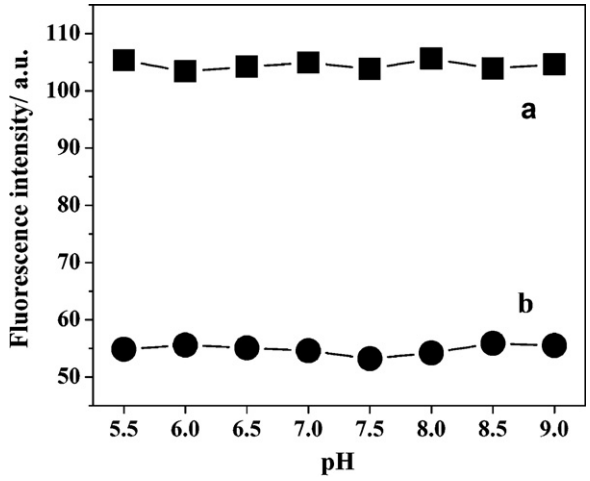

Fig. 3. Fluorescence intensity of (a) $(LDH/ANTS)_{20}$ UTF and (b) $(LDH/ANTS)_{20}$ UTF in the presence of dextran-40 as a function of pH.

and biological usage. For facile application, pH 7.0 is chosen in the subsequent study.

3.3.2. Detection for dextran-40

To investigate the fluorescence response of the $(LDH/ANTS)_{20}$ UTF sensor toward dextran-40, the fluorescence spectra of $(LDH/ANTS)_{20}$ UTF before and after the addition of dextran-40 solutions (concentration range from 1.0×10^{-5} to 1.0×10^{-2} M) are shown in Fig. 4A. A significant decrease in fluorescence intensity of $(LDH/ANTS)_{20}$ UTF was observed upon increasing dextran-40 concentration. A linear relationship between the fluorescence intensity and the concentration of dextran-40 ($-\log c$) was obtained (Fig. 4B), with the following linear regression equation: $I = 0.732 + 0.131 \log c$(dextran-40), $R^2 = 0.999$. The absolute detection limit was 2.7×10^{-6} M.

3.3.3. Selectivity

Dextran-40, glucose, fructose and sucrose are important saccharides, which generally coexist in body fluids. It is therefore of great interest to learn how these saccharides interfere the response of $(LDH/ANTS)_{20}$ UTF toward dextran-40. Fig. 5A illustrates the

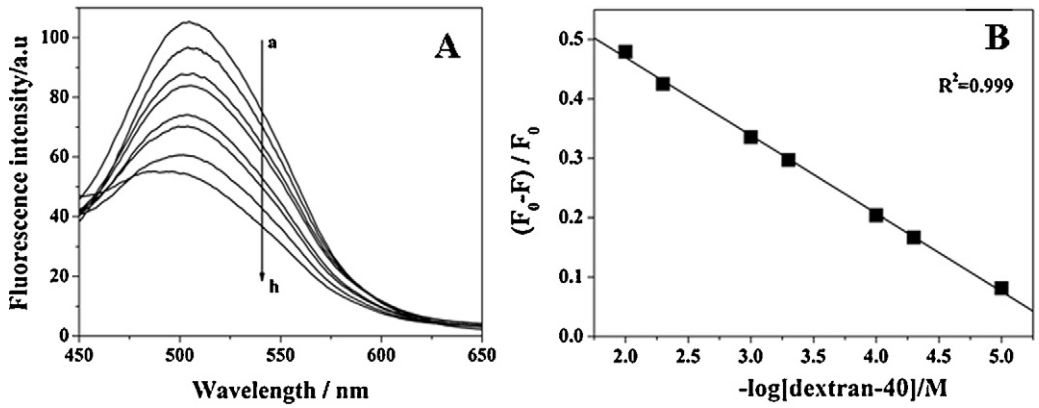

Fig. 4. (A) Fluorescence spectra of the $(LDH/ANTS)_{20}$ UTF chemosensor after immersion into aqueous solutions with different concentration of dextran-40 (λ_{ex} = 365 nm, λ_{em} = 505 nm, pH = 7.0): (a) [dextran-40] = 0 M, (b) 1.0×10^{-5} M, (c) 5.0×10^{-5} M, (d) 1.0×10^{-4} M, (e) 5.0×10^{-4} M, (f) 1.0×10^{-3} M, (g) 5.0×10^{-3} M and (h) 1.0×10^{-2} M) and (B) plot of the fluorescence intensity as a function of dextran-40 concentration.

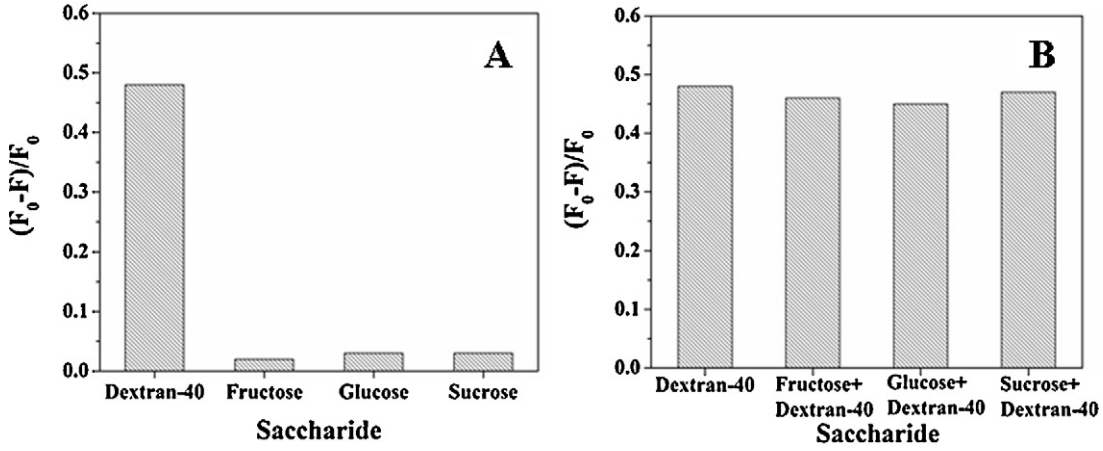

Fig. 5. (A) Fluorescence intensity changes ($[F_0 - F]/F_0$) of $(LDH/ANTS)_{20}$ UTF upon addition of dextran-40, fructose, glucose and sucrose, respectively (the concentration of saccharides is 1.0×10^{-3} M) and (B) fluorescence intensity changes ($[F_0 - F]/F_0$) of $(LDH/ANTS)_{20}$ UTF upon addition of dextran-40 in the presence of fructose, glucose and sucrose (5.0×10^{-3} M).

fluorescence intensity change of $(LDH/ANTS)_{20}$ UTF toward various saccharides, respectively. Remarkably, no optical intensity change was observed before and after the addition of the saccharides except dextran-40. The results demonstrated that the $(LDH/ANTS)_{20}$ UTF can be used as a chemosensor for selective detection of dextran-40 over a range of other saccharides. In addition, the fluorescence response of the UTF toward dextran-40 in the presence of other saccharides is investigated. Fig. 5B shows the fluorescence intensity change of $(LDH/ANTS)_{20}$ UTF for detecting dextran-40 (5.0×10^{-3} M) in the presence of other saccharides (5.0×10^{-3} M), in which no significant variation in fluorescence intensity was found with the interference of saccharides. The results demonstrate that the $(LDH/ANTS)_{20}$ UTF possesses a high selectivity for dextran-40.

3.3.4. The regeneration and reversibility

It has been reported that H_2O_2 can be used as an oxidation in chemical regeneration of oligosaccharides from their fluorescent derivatives by the reductive amination reaction [23]. Therefore, the regeneration of $(LDH/ANTS)_{20}$ UTF was performed by immersing the quenched $(LDH/ANTS)_{20}$ UTF into a solution of H_2O_2 (1.0×10^{-4} M). Fig. 6 displays the reversibility (reusability) of the sensor for dextran-40. The film was alternately exposed to the dextran-40 solution (1.0×10^{-3} M) and H_2O_2 solution

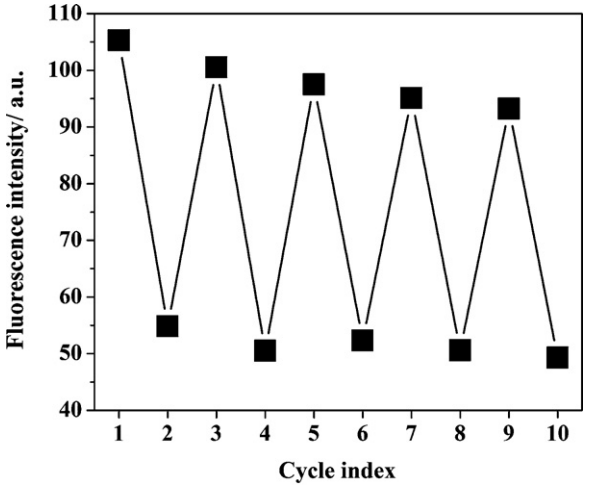

Fig. 6. Fluorescence intensity of $(LDH/ANTS)_{20}$ UTF after alternate treatment by aqueous solution of dextran-40 (1.0×10^{-3} M) and H_2O_2 (1.0×10^{-4} M), respectively (λ_{ex} = 365 nm).

(1.0×10^{-4} M), and the corresponding fluorescence emission at 505 nm was measured every 2 min. It was found the $(LDH/ANTS)_{20}$ UTF shows a good reusable ability for dextran-40, and the relative standard deviation was calculated to be 4.84% (H_2O_2) and 4.18% (dextran-40) for 10 cycles. When the quenched film was exposed

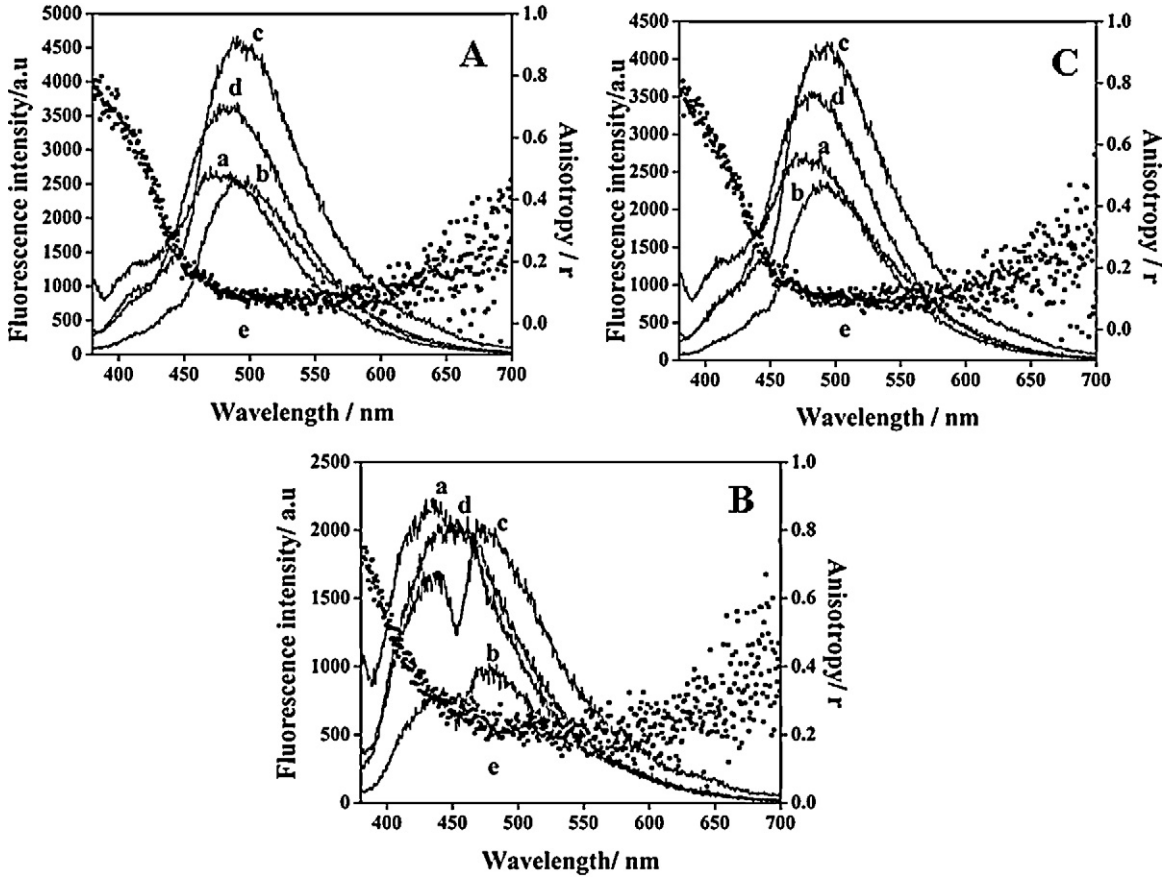

Fig. 7. Photoemission profiles in the (a) VV, (b) VH, (c) HV, (d) HH, (e) polarizations and anisotropy of the sample measured at room temperature (293 K): (A) the original $(LDH/ANTS)_{20}$ UTF, (B) the $(LDH/ANTS)_{20}$ UTF after the measurement of dextran-40 and (C) the regenerated $(LDH/ANTS)_{20}$ UTF by H_2O_2 solution. (VH stands for the PL intensity obtained with vertical polarized light excitation and horizontal polarization detection, and VV, HV, HH are defined in a similar way.)

to H_2O_2 solution, the dextran-40 and ANTS were separately recovered by H_2O_2 oxidation, accounting for the regeneration of $(LDH/ANTS)_{20}$ UTF.

3.3.5. Mechanism of the detection of dextran-40

In order to give a further insight into the mechanism of measurement-regeneration cycle, the polarized photoemission spectra of the original $(LDH/ANTS)_{20}$ UTF, the quenched and recovered UTF samples were measured and displayed in Fig. 7. The measurement of the anisotropic value r is often used to evaluating fluorescence polarization, which was fully described by Valeur [24]. For the original $(ABTS/LDH)_{20}$ UTF, it shows well-defined fluorescence anisotropy with the anisotropy value r of 0.11 (Fig. 7A) due to the ordered arrangement of ANTS. After the measurement of dextran-40 (Fig. 7B), the anisotropy value r increased dramatically from 0.11 to 0.23. This may indicate that the mobility of ANTS (vibration and rotation) was restricted by its reaction to dextran-40, resulting in the enhancement of anisotropy. After regeneration by H_2O_2 solution, the fluorescence anisotropy value decreased to 0.12 again (Fig. 7C), owing to the removal of dextran-40 from the $(LDH/ANTS)_{20}$ UTF.

The interaction between the $(LDH/ANTS)_{20}$ UTF and dextran-40 was also probed by using C 1s and N 1s XPS spectroscopy (Fig. 8A and B). Compared with the original $(LDH/ANTS)_{20}$ UTF (Fig. 8A(a)), the XPS spectrum of C 1s after measurement of dextran-40 displays a new peak attributed to C—O—H (286.4 eV, Fig. 8A(b)), indicating that dextran-40 was bonded in the UTF [25]. The disappearance of C—O—H signal for the regenerated UTF by H_2O_2 confirms the removal of dextran-40 from the UTF (Fig. 8A(c)). In addition, the XPS of N 1s (399.6 eV and 402.0 eV, Fig. 8B(b)) for the quenched $(LDH/ANTS)_{20}$ UTF have a decreased shift compared with those of original (400.1 eV and 402.5 eV, Fig. 8B(a)) and regenerated one (399.8 eV and 402.4 eV, Fig. 8B(c)), suggesting that N atom in ANTS may be complexed to C atom in dextran-40. Therefore, the XPS results indicate the interaction between dextran-40 and the sensor film.

More structural details of interaction between $(LDH/ANTS)_{20}$ UTF and dextran-40 can be deduced from the Raman spectroscopy. Fig. 8C represents the Raman spectra of the original $(LDH/ANTS)_{20}$ UTF, the quenched $(LDH/ANTS)_{20}$ UTF, and the regenerated UTF. Compared with original and regenerated $(LDH/ANTS)_{20}$ UTF (Fig. 8C(a) and (c)), the quenched $(LDH/ANTS)_{20}$ UTF (Fig. 8C(b)) shows the band at 1064 cm^{-1} which is attributed to the group of C—O. The band of C—N shifts from 1368 cm^{-1} to 1358 cm^{-1}, indicating the interaction between N atom in $(LDH/ANTS)_{20}$ UTF and C atom in dextran-40. It is concluded that dextran-40 was bonded within the UTF via the complexation with ANTS.

On the basis of the above results and enlightened by previous studies about the chemical reactions of ANTS with saccharides [26], we propose a response mechanism of LDH/ANTS UTF toward dextran-40 as shown in Scheme 1B.

3.4. Analytical application

To explore the potential of $(LDH/ANTS)_{20}$ UTF for practical applications, we checked the feasibility of using $(LDH/ANTS)_{20}$ UTF for detection of dextran-40 under the simulated physiological conditions (Fig. 9). The simulated physiological solution is a phosphate buffered solution (PBS) with 100 mM NaCl to keep constant ionic strength. From the Fig. 9, it can be seen that addition of dextran-40

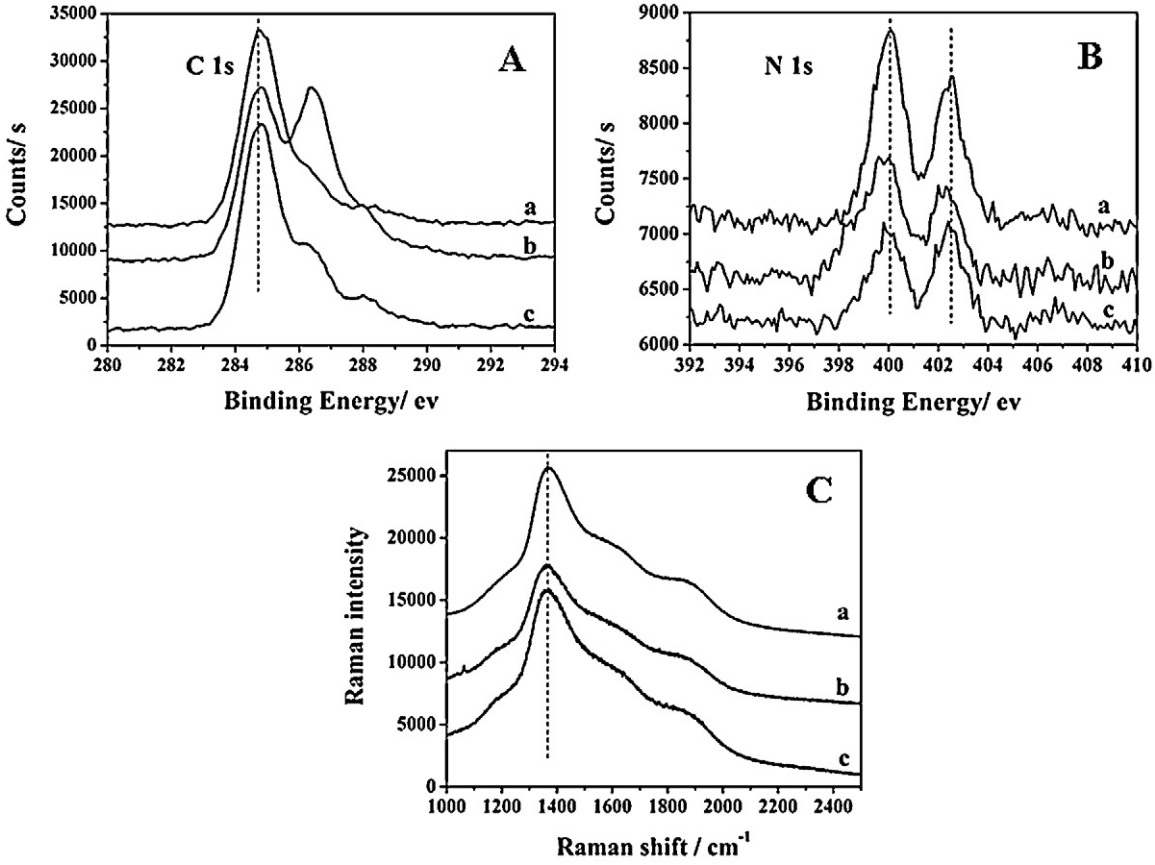

Fig. 8. The XPS spectra (A), (B) and the Raman spectra (C): the original $(LDH/ANTS)_{20}$ UTF (a), the UTF after measurement of dextran-40 (b) and the regenerated UTF by H_2O_2 solution (c).

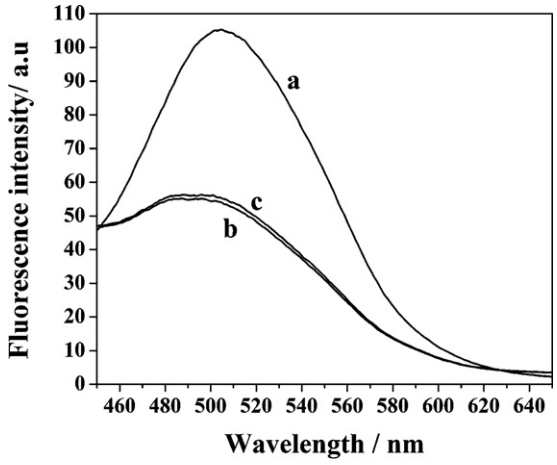

Fig. 9. The fluorescence spectra of (a) the $(LDH/ANTS)_{20}$ UTF, (b) the $(LDH/ANTS)_{20}$ UTF upon addition of dextran-40 solution and (c) upon addition of dextran-40 in the simulated physiological condition.

in an artificial physiological solution quenched the fluorescence of $(LDH/ANTS)_{20}$ UTF, which is very close to the response behavior of the pure dextran-40 solution.

4. Conclusions

In this study, we have explored a facile, efficient, and economical route to obtain the $(LDH/ANTS)_n$ UTFs, and its selective recognition toward dextron-40 was investigated. UV–vis spectroscopy, fluorescence spectroscopy, XRD, SEM and AFM have been adopted to characterize the assembly process, and the sensing response of the $(LDH/ANTS)_{20}$ UTF toward dextran-40 was studied in detail by using the fluorescence spectroscopy. It was found that the $(LDH/ANTS)_{20}$ UTF can be used for dextran-40 sensing in the concentration range 1.0×10^{-5} to 1.0×10^{-2} M, and the detection limit of 2.7×10^{-6} M is obtained. Good selectivity toward dextran-40 over other saccharides (glucose, fructose and sucrose) has also been demonstrated. In addition, the mechanism of the $(LDH/ANTS)_{20}$ UTF for determination of dextran-40 was revealed by a combination study based on the polarized photoemission, XPS and Raman spectroscopy, from which the strong interaction between dextran-40 and ANTS occurs and is responsible for the significant fluorescence quenching. Therefore, this work provides a facile and efficient strategy for the immobilization of organic molecule into an inorganic matrix, which can be potentially applied for the selective detection of dextran-40. We will also work on expanding the scope of applications of the ultrathin film into other types of dextran, and other molecules of biological importance.

Acknowledgments

This project was supported by the National Natural Science Foundation of China, the 863 Program (Grant No. 2009AA064201) and the Cooperative Special Program of Beijing.

Appendix A. Supplementary data

Supplementary data associated with this article can be found, in the online version, at http://dx.doi.org/10.1016/j.snb.2012.10.105.

References

[1] P.J. Garegg, Saccharides of biological importance: challenges and opportunities for organic synthesis, Accounts of Chemical Research 25 (1992) 575–580.
[2] A.P. Davis, R.S. Wareham, Carbohydrate recognition through noncovalent interactions: a challenge for biomimetic and supramolecular chemistry, Angewandte Chemie International Edition 38 (1999) 2978–2996.
[3] J.Y. Yoon, A.W. Czarnik, Fluorescent chemosensors of carbohydrates: a means of chemically communicating the binding of polyols in water based on chelation-enhanced quenching, Journal of the American Chemical Society 114 (1992) 5874–5875.
[4] Y. Liu, C. Deng, L. Tang, A.J. Qin, R.R. Hu, J.Z. Sun, B.Z. Tang, Specific detection of D-glucose by a tetraphenylethene-based fluorescent sensor, Journal of the American Chemical Society 133 (2011) 660–663.
[5] T.I. Ishi, M.A.T. Mateos, P. Timmerman, M.C. Crego, D.N. Reinhoudt, S. Shinkai, Self-assembled receptors that stereoselectively recognize a saccharide, Angewandte Chemie International Edition 42 (2003) 2300–2305.
[6] T. Levy, C. Déjugnat, G.B. Sukhorukov, Polymer microcapsules with carbohydrate-sensitive properties, Advanced Functional Materials 18 (2008) 1586–1594.
[7] C.J. Musto, K.S. Suslick, Differential sensing of sugars by colorimetric arrays, Current Opinion in Chemical Biology 14 (2010) 758–766.
[8] B. Vilozny, A. Schiller, R.A. Wessling, B. Singaram, Multiwell plates loaded with fluorescent hydrogel sensors for measuring pH and glucose concentration, Journal of Materials Chemistry 21 (2011) 7589–7595.
[9] G. Fukuhara, Y. Inoue, Highly selective oligosaccharide sensing by a curdlan–polythiophene hybrid, Journal of the American Chemical Society 133 (2011) 768–770.
[10] K. Nilsson, G. Söderlund, Clinical dextrans: specifications and quality of preparations on the market, Acta Pharmaceutica Suecica 15 (1978) 439–454.
[11] R.M. Alsop, G.J. Vlachogiannis, Determination of the molecular weight of clinical dextran by gel permeation chromatography on TSK PW type columns, Journal of Chromatography A 246 (1982) 227–240.
[12] C. Laura, G. Maria, S. Po-Wah, Glycans in magnetic resonance imaging: determinants of relaxivity to smart agents and potential applications in biomedicine, Current Medicinal Chemistry 18 (2011) 1002–1018.
[13] Y. Oonuki, Y. Yoshida, Y. Uchiyama, A. Asari, Application of fluorophore-assisted carbohydrate electrophoresis to analysis of disaccharides and oligosaccharides derived from glycosaminoglycans, Analytical Biochemistry 343 (2005) 212–222.
[14] G.L. Huang, H.C. Zhang, P.G. Wang, The analysis of oligosaccharides derived from different sources by fluorophore-assisted carbohydrate electrophoresis, Food Chemistry 101 (2007) 392–396.
[15] X. Li, J.P. Liu, X.X. Ji, J. Jiang, R.M. Ding, Y.Y. Hu, A.Z. Hu, X.T. Huang, Ni/Al layered double hydroxide nanosheet film grown directly on Ti substrate and its application for a nonenzymatic glucose sensor, Sensors and Actuators B: Chemical 147 (2010) 241–247.
[16] A.I. Khan, D. O'Hare, Intercalation chemistry of layered double hydroxides: recent developments and applications, Journal of Materials Chemistry 12 (2002) 3191–3198.
[17] M.S. Lopez, F. Leroux, C. Mousty, Amperometric biosensors based on LDH-alginate hybrid nanocomposite for aqueous and non-aqueous phenolic compounds detection, Sensors and Actuators B: Chemical 150 (2010) 36–42.
[18] J.H. Choy, J.S. Jung, J.M. Oh, M. Park, J.Y. Jeong, Y.K. Kang, O.J. Han, Layered double hydroxide as an efficient drug reservoir for folate derivatives, Biomaterials 25 (2004) 3059–3064.
[19] Z.Y. Sun, L. Jin, W.Y. Shi, M. Wei, D.G. Evans, X. Duan, Controllable photoluminescence properties of an anion-dye-intercalated layered double hydroxide by adjusting the confined environment, Langmuir 27 (2011) 7113–7120.
[20] Q. Wang, D. O'Hare, Recent advances in the synthesis and application of layered double hydroxide (LDH) nanosheets, Chemical Reviews 112 (2012) 4124–4155.
[21] R. Ma, Z. Liu, L. Li, N. Iyi, T. Sasaki, Exfoliating layered double hydroxides in formamide: a method to obtain positively charged nanosheets, Journal of Materials Chemistry 16 (2006) 3809–3813.
[22] R.P. Bontchev, S. Liu, J.L. Krumhansl, J. Voigt, Synthesis characterization, and ion exchange properties of hydrotalcite $Mg_6Al_2(OH)_{16}(A)_x(A')_{2-x}{\cdot}4H_2O$ (A, A′ = Cl^-, Br^-, I^-, and NO_3^-, $2 \geq x \geq 0$) derivatives, Chemistry of Materials 15 (2003) 3669–3675.
[23] S. Suzuki, T. Fujimori, M. Yodoshi, Recovery of free oligosaccharides from derivatives labeled by reductive amination, Analytical Biochemistry 354 (2006) 94–103.
[24] B. Valeur, Molecular Fluorescence: Principles and Applications, Wiley-VCH, Verlag, 2001.
[25] S. Stankovich, R.D. Piner, X. Chen, N. Wu, S.T. Nguyen, R.S. Ruoff, Stable aqueous dispersions of graphitic nanoplatelets via the reduction of exfoliated graphite oxide in the presence of poly(sodium 4-styrenesulfonate), Journal of Materials Chemistry 16 (2006) 155–158.
[26] F.Y. Che, J.F. Song, R. Zeng, K.Y. Wang, Q.C. Xia, Analysis of 8-aminonaphthalene-1,3,6-trisulfonate-derivatized oligosaccharides by capillary electrophoresis–electrospray ionization quadrupole ion trap mass spectrometry, Journal of Chromatography A 858 (1999) 229–238.

Biographies

Lan Jin received her PhD from Nanjing University in 1997, and was a postdoctoral researcher at Nankai University from 1998 to 2000. She worked as an associate professor in the College of Science in Beijing University of Chemical Technology in 2000. Her main research interests involve the preparation of functional organic–inorganic composite materials, molecular recognition in supramolecular chemistry, and their application in environmental, biosensors and biomedicine.

Zhijie Guo is a master student in the College of Science, Beijing University of Chemical Technology. Her research interest is fabricating inorganic–organic composite film for various sensing applications.

Tengli Wang is a master student in the College of Science, Beijing University of Chemical Technology. His research interest is fabricating inorganic–organic composite film for various biosensing applications.

Min Wei received her PhD from Peking University in 2001. She is a full professor in the State Key Laboratory of Chemical Resource Engineering and the College of Science in Beijing University of Chemical Technology. Her main research interests are in supramolecular assembly chemistry, functional intercalated materials, and the development of organic–inorganic photoluminescence film materials.